Modeling driver steering behavior in restricted-preview boundary-avoidance tasks

van der El, Kasper; Pool, Daan M.; van Paassen, Marinus M.; Mulder, Max

DOI
10.1016/j.trf.2023.02.017

Publication date
2023

Document Version
Final published version

Published in
Transportation Research Part F: Traffic Psychology and Behaviour

Citation (APA)
van der El, K., Pool, D. M., van Paassen, M. M., & Mulder, M. (2023). Modeling driver steering behavior in restricted-preview boundary-avoidance tasks. *Transportation Research Part F: Traffic Psychology and Behaviour*, *94*, 362-378. https://doi.org/10.1016/j.trf.2023.02.017

Transportation Research Part F: Psychology and Behaviour 94 (2023) 362–378

Contents lists available at ScienceDirect

Transportation Research Part F: Psychology and Behaviour

journal homepage: www.elsevier.com/locate/trf

Modeling driver steering behavior in restricted-preview boundary-avoidance tasks

Kasper van der El, Daan M. Pool *, Marinus M. van Paassen, Max Mulder

Control and Simulation, Aerospace Engineering, Delft University of Technology, Delft, the Netherlands

ARTICLE INFO

Keywords:
Driver behavior
Driver modeling
Preview
Reduced visibility
Steering

ABSTRACT

In the design of human-like steering support systems, driver models are essential for matching the supporting automation's behavior to that of the human driver. However, current driver models are very limited in capturing the driver's adaptation to key task variables such as road width and visibility (i.e., '*preview*' of the road ahead). This paper uses a recently proposed, novel control-theoretical model for centerline tracking to investigate driver steering in lane-keeping tasks with restricted and unrestricted preview, in an attempt to substantially extend this model's validity. Using data from a tailored driving simulator experiment, three driver control loops (feedforward, heading and position feedback) are separately quantified using system identification techniques. The results show that when preview is restricted, drivers use all of the remaining preview to anticipate the curves of the road ahead, and are no longer able to 'smooth' tight curves in the road trajectory (i.e., corner cutting). When sufficient preview and lane width are available, the time to line crossing increases, and steering behavior is less aggressive and more intermittent, or more 'satisficing'. The novel driver steering model captures these adaptations very well (over 95% of the steering actions) and can thereby be instrumental in realizing human-like steering automation and support systems.

1. Introduction

The rise of automation in automotive technology, from advanced driver assistance systems (ADAS) to self-driving cars, holds a huge promise for lower accident numbers and improving safety in general. Across many domains where similar automation trends can be observed, e.g., in manufacturing, industry, on board aircraft and in air traffic control, an important requirement for the design and use of automation will be whether human operators trust and accept it. An avenue to improve driver acceptance of automation is to design that automation such that it behaves in a reliable, predictable, and even a 'human-like' way (Schnelle et al., 2018, Saleh et al., 2011, Wang et al., 2022, Mulder et al., 2018). For this purpose it is important to understand, and be able to predict, how drivers behave in – and *adapt* to changes in – particular circumstances, such as road geometry, delineation, and visibility of the road ahead (Barendswaard et al., 2019, Weir & McRuer, 1973). Ideally, the automation would then behave and adapt in a similar way as the driver would do, building driver trust in the automation's capabilities (Mars, 2008, Mulder et al., 2018).

Mathematical models of driver behavior can be extremely helpful in designing, tuning, testing and evaluating vehicle automation. The ability to objectively describe and quantify the driver dynamic response in similar terms as the automation being designed has been an important motivation for research since the 1960s. A plethora of driver models have been developed and published, ranging

* Corresponding author.
E-mail address: d.m.pool@tudelft.nl (D.M. Pool).

https://doi.org/10.1016/j.trf.2023.02.017
Received 4 October 2021; Received in revised form 30 November 2022; Accepted 8 February 2023

Available online 14 March 2023

from a broad set of classical control-theoretical models (Weir & McRuer, 1970, McRuer et al., 1977, Allen et al., 1977, Donges, 1978, MacAdam, 2003, Saleh et al., 2011) to models based on adaptive predictive control (Ungoren & Peng, 2005), hierarchical concurrent state machines (Demir & Cavusoglu, 2012), optimal linear preview control (Odhams & Cole, 2014), QN-ACTR control (Deng et al., 2019, Li et al., 2020), optical cue-based control (Kovakova et al., 2020), and sliding mode control (Zhu & He, 2020). The ultimate goal is to have a model as part of the support or automation system that identifies (changes in) driver behavior in real-time, to directly update the parameters of an 'internal' control-theoretical model (McRuer et al., 1975) or to be able to categorize changes between different steering strategies (Barendswaard et al., 2019).

This paper extends on a recently proposed unified driver model which originates from fundamental research studying how human controllers use preview of the target trajectory ahead in time (van der El, Pool, & Mulder, 2019, van der El et al., 2020). The model focuses on the *lane keeping task* and has a number of key advantages: (i) it is relatively simple, as it is based on classical quasi-linear manual control theory, extending earlier work (McRuer et al., 1975, van der El, Pool, et al., 2018), (ii) its loop closures and parameters can be physically interpreted, as they are based on variables that the driver can see ahead, (iii) its parameters can be objectively identified from experimental data, (iv) it has been shown to be able to explain and predict 95% of observed human control behavior in a variety of settings (van der El, Pool, & Mulder, 2019, van der El et al., 2020). A current limitation of the model is that it has not been demonstrated to also account for driver adaptation to crucial task variables such as driving velocity, visibility (preview), and lane width. In this paper, the model will be applied to study how drivers adapt their lane keeping behavior to two crucial task variables. First, the available *preview* of the road ahead, i.e., the effects of visibility in driving, simulated with computer-generated fog. Second, the *task instruction*, that is, the instruction to either drive exactly along the road center, or keep the car in the driving lane (i.e., "drive as one normally would"), simulated with presenting, respectively, only the road centerline or the road boundaries.

Such model-based analysis traditionally relies heavily on frequency-domain measures (Weir & McRuer, 1970, van der El, Pool, & Mulder, 2019). However, in the literature on driving often more readily interpretable time-domain measures are used, such as the '*time to line crossing*' (TLC), see e.g., Godthelp et al. (1984), Godthelp (1986), Reymond et al. (2001), Xu et al. (2015), Wolters et al. (2018). A secondary goal of this paper is to connect the model-based and frequency-domain results (van der El, Pool, & Mulder, 2019, van der El et al., 2020), to such time-domain measures. To do so, new empirical human-in-the-loop steering data are presented. These data were collected in a simulator driving experiment, with the specific purpose to facilitate analyzing the driver's adaptation both in the time- and frequency-domain, as well as by identifying the parameters in the control-theoretic driver model from van der El et al. (2020).

The contributions of this paper are as follows. A novel control-theoretical driver model is presented that allows for an objective description and prediction of driver control behavior adaptations to preview and task instruction. The model unifies existing driver models and theories of driver perception and will be verified in a realistic simulated environment; its parameters can be physically interpreted and linked to vehicle dynamics and visual scene properties; the control-theoretical insights (mostly in the frequency domain) will be linked to more commonly used time-domain behavioral metrics. The relevance of the paper lies in the potential use of the model in designing ADAS for steering (e.g., lane keeping assist), the acceptance of which depends on the ability to adapt to changes in the available preview ahead (limited visibility, fog) in ways drivers will understand, appreciate, and trust.

The paper is structured as follows. In Section 2 the essential background literature on driver steering behavior and the control-theoretic driver model of van der El et al. (2020) will be summarized. This includes how the cues available in the driver's visual field are captured by the model. We then proceed with explaining the experiment performed to identify the driver model parameters in Section 3. The results are presented in detail in Section 4 and discussed in Section 5. The paper ends with conclusions and recommendations for future work in Section 6.

2. Background

2.1. Literature

2.1.1. Available preview

Human and automated controllers can benefit profoundly from the availability of preview information about the target trajectory to follow in the near future (e.g., see Weir & McRuer, 1970, McRuer et al., 1977, Allen et al., 1977, Donges, 1978, MacAdam, 2003, Saleh et al., 2011, McLean & Hoffmann, 1973, Hess & Modjtahedzadeh, 1989). Both stability and performance metrics deteriorate when preview is restricted, which has been shown, for example, when driving through fog on a winding road (McLean & Hoffmann, 1973, Allen et al., 1977, Allen & O'Hanlon, 1979, Land & Horwood, 1995a, van der Hulst et al., 1998) and when the available preview is limited on tracking displays, e.g. van der El, Padmos, et al. (2018). Experiments with single-loop tracking tasks and quasi-linear control models revealed that restricted preview does not only limit the human's abilities to anticipate, as reported in driving (van der Hulst et al., 1998), but also to *smooth* the target trajectory ahead, that is, to effectively filter-out the higher-frequency components of the road ahead, see van der El, Padmos, et al. (2018), van der El et al. (2020). Although restricted preview has an equivalent negative effect on centerline-tracking *performance* in steering of ground vehicles such as passenger cars, it is as of yet unclear whether humans adapt their *control behavior* identically in these more realistic tasks.

2.1.2. Driving speed

Much of the literature on the effects of reduced visibility (preview) on driver behavior focuses on speed adaptation in fog, and not on changes in behavior when it comes to the task of lane-keeping (i.e., steering). To reduce risk, drivers are known to lower their speed and increase time headway to other vehicles when visibility reduces (van der Hulst et al., 1998, Broughton et al., 2007, Caro

et al., 2009, Yan et al., 2014, Li et al., 2015, Siebert & Wallis, 2019, Huang et al., 2020, Zolali & Mirbaha, 2020). Speed reductions also occur as a function of curve radius (slower in steeper curves) and curve deflection (van Winsum & Godthelp, 1996, Bella et al., 2014), and experienced drivers have been shown to drive faster in clear visibility, compared to novice drivers, but slower in reduced visibility (Mueller & Trick, 2012). Whereas van der Hulst et al. (1998) found that when speed compensation was not possible drivers simply have to maintain high alertness (to react to unpredictable events), Brooks et al. (2011) showed that drivers do not tend to slow down significantly until visibility distance is drastically reduced, and lane keeping ability is maintained until fog results in visibility distances less than 30 meters.[1] Naturally, these results all depend heavily on the presence and predictability of traffic (or obstacles) ahead, as when no traffic is ahead the driver can focus mainly on following the road, possibly at higher speeds as there is no risk of collision.

2.1.3. Lane keeping

When the nature of the driving task is studied, it is clear that instead of tracking an exactly defined target trajectory (e.g., the road centerline), a range of lateral positions between the demarcated lane edges is equally acceptable: lane-keeping is essentially a boundary-avoidance task (Godthelp, 1986, Mammer et al., 2006, Boer, 2016). Tracking tasks require continuous attention and control from the operator, and changes in the target signal, external disturbances, and internal perception or motor noise directly yield 'errors' and thus an incentive to steer (Mulder et al., 2018).

In contrast, in boundary-avoidance tasks deviations from the centerline are not considered errors per se; such deviations may accumulate over time, before evoking a control response only after passing a certain threshold. In this respect, the phenomenon of corner cutting is often a manifestation of driving skill, and not control error (Boer, 2016). Experimental data suggest that drivers aim to keep the '*time to line crossing*' (TLC), that is, the time before the vehicle would leave the road assuming constant control inputs, above a threshold of 3-4 s (Godthelp, 1986). The TLC quantifies the time available to the driver to make a corrective steering action; sufficiently high TLCs evoke no steering response and can even lead to intermittent control (Godthelp et al., 1984, Godthelp, 1986, Markkula et al., 2018). As opposed to tracking, such human behavior has been quite generally referred to as error-neglecting (Godthelp, 1986), boundary-avoidance (Gray, 2005, 2008, Mammer et al., 2006, Padfield et al., 2012), or – as will be used here – *satisficing* control (Boer, 2016).

It is important to distinguish the control task from the human's behavior. Boundary-avoidance tasks may still evoke tracking behavior, for example, narrower road lanes were shown to lead to smaller deviations from the centerline in driver steering tasks (McLean & Hoffmann, 1972), and also from the tunnel center when flying through a virtual tunnel-in-the-sky (Mulder & Mulder, 2005). Vice versa, operators may (temporarily) adopt satisficing behavior in tracking tasks, for example, when prioritizing lower control effort.

2.1.4. Visual field

Most if not all driver model-based investigations referred to above have shown that drivers adopt a multiloop control organization, exploiting preview/feedforward information about the future road curvature, as well as feedback signals about both lateral position and heading, see Weir and McRuer (1973), McRuer et al. (1977). Information-centered studies revealed the richness of information from the outside visual scene, including the optical flow caused by the vehicle motion (see e.g., Gordon, 1965, 1966a, 1966b). Pioneering work by Grunwald and Merhav (1976) showed that in following a reference trajectory in three-dimensional space, the visual scene can be separated in two regions. The 'far field' provides information about the vehicle's heading (direction of motion) relative to the (possibly curved) trajectory, whereas the 'near field' provides information about the vehicle's position relative to the reference trajectory. These elementary geometrical motion mapping relationships can explain the landmark studies on driver perception published twenty years later by Land and Lee (1994), Land and Horwood (1995b), which showed that driver lane keeping performance indeed depends on what parts of the outside visual field are available.

2.2. Model rationale

Multiloop control-theoretical driver models exist since the mid-1960s (Weir & McRuer, 1970) (Donges, 1978) and have often been tuned, modified and expanded ever since. Most if not all of these models have in common that they capture at least the two essential loops to be closed by the driver, that of the vehicle heading and its lateral position on the road. Most models are constructed as a combined feedforward (on future road curvature or position) and feedback (on heading error and position error) control structure. The vehicle 'states' (heading, position) and road characteristics (curvature, look-ahead) are typically assumed to be 'known' or 'perceived' by the driver, without much detail on how exactly these are perceived from the outside visual scene. Similarly, much literature exists on what visual cues the driver can use, see Gordon (1965, 1966a, 1966b) for some early examples, without specifying what feedback loops may result from perceiving them (Mulder & Mulder, 2005).

van der El et al. (2020) proposed a new theory of driver steering, which aims to unify visual perception and control models. For a detailed description of this model the reader is referred to this previous paper, here only the main elements will be explained at the hand of Fig. 1 and Fig. 2. Fig. 1 shows a typical, straight-ahead, frontal view from a car's windshield, with a winding road ahead (curved black lines) and the car's predicted future path in gray. With unrestricted visibility the driver can see ahead up until the horizon line (note that we assume a flat surface), but when preview is restricted we model this with the time constant τ_p: beyond this time (indicated by the horizontal black dashed line in Fig. 1) the road ahead is not visible.

[1] Corresponding to approx. 1.2 seconds visible preview ahead (velocity ≈ 89 m/s).

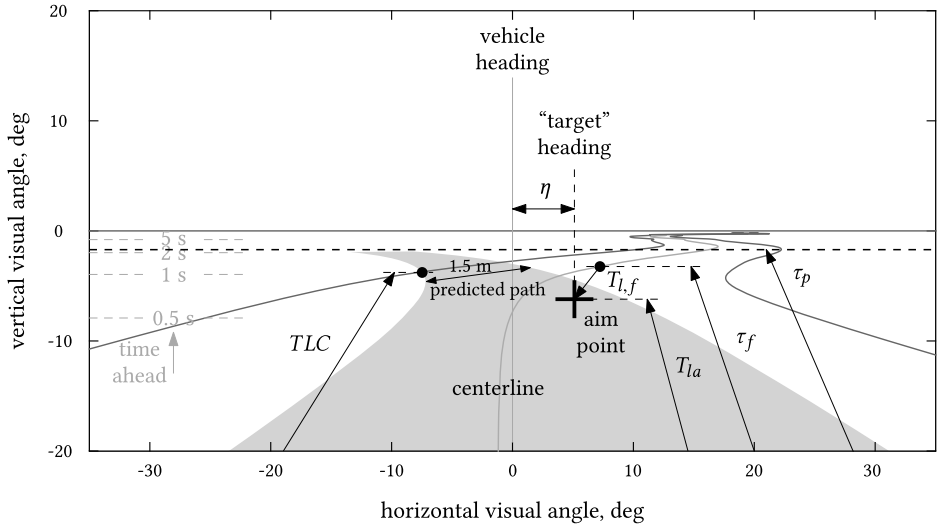

Fig. 1. Illustration of physical meaning of the model's look-ahead times, together with the visual angle η that is effectively minimized by the driver through compensatory control.

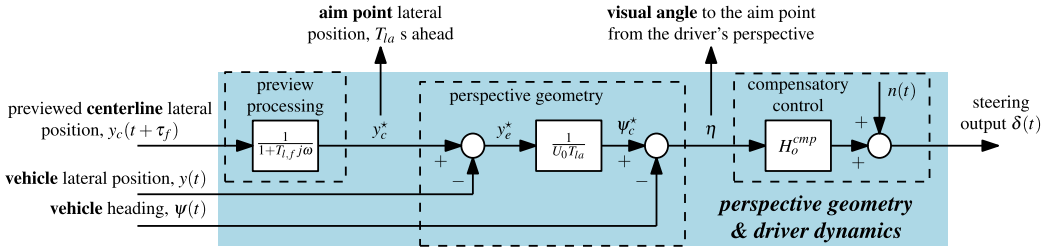

Fig. 2. Multiloop driver steering model, combining visual feedback selection and control.

The essence of the model lies in the fact that it assumes the driver, when following curved or straight roads, to use the preview ahead of the car to self-generate an 'aim-point' some distance or time ahead of the car, and then minimize the visual angle η between the aim-point heading and the current vehicle heading ψ. This is further illustrated in Fig. 2, which shows the multiloop driver model with three inputs: (i) the previewed road centerline lateral position τ_f seconds ahead ($y_c(t+\tau_f)$), (ii) the current lateral position ($y(t)$), and (iii) the heading of the vehicle $\psi(t)$. The model assumes the driver to 'smooth' the previewed road centerline ($y_c(t+\tau_f)$) through low-pass filtering with a time constant of $T_{l,f}$ seconds. This effectively places that point $T_{l,f}$ seconds closer to the driver, yielding an aim point lateral position $y_c^\star$ with 'look-ahead time' $T_{la} = \tau_f - T_{l,f}$ in seconds ahead. Applying perspective geometry, using the current lateral position and the effective distance ahead to the aim point ($U_0 T_{la}$, with U_0 the vehicle velocity in m/s), yields the 'target heading' $\psi_c^\star$ of that aim point. Then, comparing this target heading with the current heading yields the visual angle η to the aim point from the driver's perspective which can be minimized through simple compensatory tracking. As in traditional quasi-linear operator models, all human behavior that is not linear time-invariant is captured by a single remnant signal $n(t)$, see for example McRuer et al. (1975). The remnant includes nonlinear and time-varying steering behavior, as well as a random component due to perception and motor noise (Levison et al., 1969, Mulder et al., 2018).

2.3. Model parameters and identifiability

An advantage of the model is that its parameters can be physically interpreted, that is, related to the view outside the car. Summarizing its main parameters, the τ_f variable indicates the farthest point of the road ahead that is used by the driver for control, which is used in two ways. The farthest $T_{l,f}$ seconds of these are used to smooth the 'oscillations' or tight curves of the trajectory ahead, such that the driver only follows the lower-frequency variations, effectively leading to behavior known as 'corner cutting'. The closest T_{la} seconds are used to anticipate on what is coming, effectively allowing the driver to compensate for the vehicle's response lag, and her or his own limitations, mainly neuromuscular actuation lags and perception, processing and actuation time delays. The compensatory control model has a traditional structure (McRuer et al., 1977) and will be explained in more detail in Section 3.5.2.

Regarding the model's identifiability, Fig. 2 shows that the driver model has three inputs, hence the driver effectively closes three loops. From a model identification perspective, using an instrumental variable technique means that three independent 'forcing functions' must be inserted in the closed-loop (van Paassen & Mulder, 1998). One is readily available, namely the trajectory of

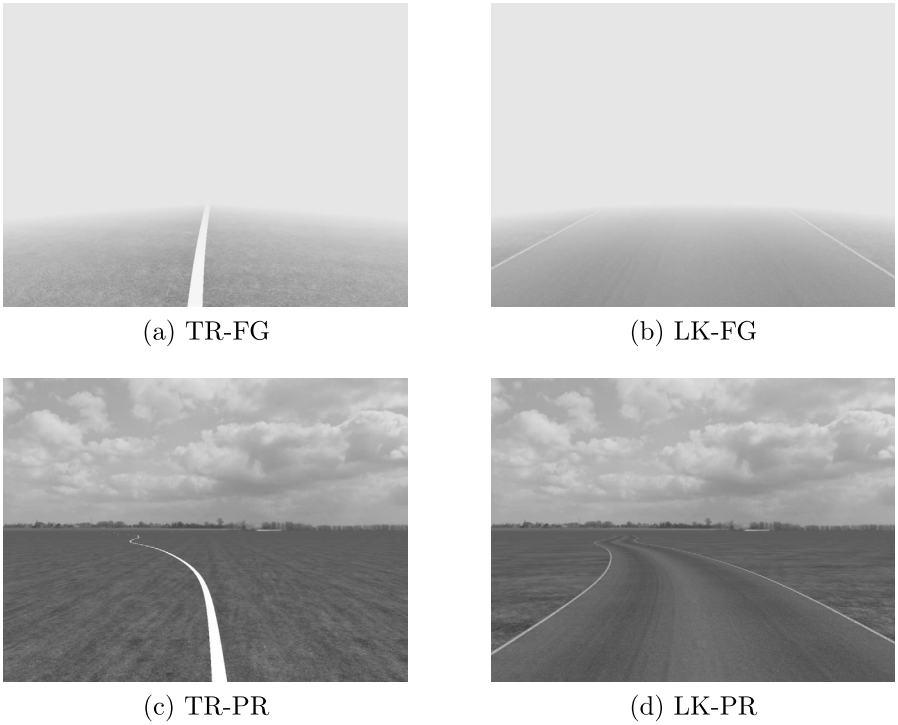

Fig. 3. Central portion of the experimental visuals as presented to the participants.

the road centerline ahead, $y_c(t)$. The other two are defined here as a direct perturbation on the vehicle's position ($y_d(t)$) and heading ($\psi_d(t)$), both artificially representing effects of wind disturbances. What results is a target-following, disturbance-rejection task, with the road trajectory $y_c(t)$ the 'target' signal, and the position and heading perturbations reflecting the disturbance signals.

In a recent paper in which we derive the novel driver model (van der El et al., 2020), we have shown that the three forcing functions can be designed as sums of 10 sine waves (yielding a total of 30 unique frequencies) to allow for estimating the three frequency response function blocks (preview processing, perspective geometry, compensatory control) in Fig. 2. In addition, for each loop closure the crossover frequency and phase margin can be estimated from the data, measures that reflect the controller's performance and stability, respectively. These nonparametric frequency-domain data then act as input for estimating the model parameters: τ_f, $T_{l,f}$, T_{la}, and the compensatory submodel parameters. How to compute these frequency-domain measures is detailed in multiple earlier papers, see for example Weir and McRuer (1970), van Paassen and Mulder (1998), van der El, Pool, van Paassen, et al. (2019), van der El et al. (2020).

3. Driving experiment

3.1. Rationale

A simulator experiment has been performed where drivers were instructed to drive along a winding road ($y_c(t)$), while two independent disturbances ($y_d(t)$ and $\psi_d(t)$) representing wind effects were present. These signals were multisines as in (van der El et al., 2020) to enable identification of the driver dynamics according to the method described in the previous section. The velocity of the car was fixed to 50 km/hour, a common speed limit for urban driving in the Netherlands. Hence, drivers performed a *fixed-paced* lane-keeping task. Participants were asked to repeatedly drive 'runs' of about 1.8 km long along the winding road to gather data for identification.

3.2. Independent variables

Two independent variables were varied in the experiment: (i) the road presentation, and (ii) the available preview, see Fig. 3. The road was presented either by its centerline only, yielding the exact same tracking task (TR) as used in (van der El et al., 2020) to derive the driver model, or by a 3.5 m wide lane, extending 1.75 m on each side of the centerline, yielding a lane-keeping task (LK). Preview was either unrestricted (PR) or limited to 7 m ($\approx$ 0.5 s) by fog (FG) ahead of the vehicle. The factorial of the two independent variables was tested, yielding four experimental conditions referred to as TR-FG, LK-FG, TR-PR, and LK-PR.

3.3. Apparatus and control variables

The experiment was performed in the SIMONA research simulator of TU Delft. The simulator has an outside visual (180x40 deg) projected on a collimated screen; no physical motion was simulated. The setup was identical to that used in (van der El et al., 2020), but with slight adaptations to better represent real-life driving tasks. First, the 'bicycle model' was used for the vehicle dynamics (Rajamani, 2011); the model parameters were configured to resemble a neutrally steering, typical passenger car, identical to Lakerveld et al. (2016). Second, the ground and sky planes of the outside scenery showed a typical rural road found in The Netherlands, identical to Wolters et al. (2018). The rich textures for the grass and clouds were absent in the experiment of van der El et al. (2020), but Wolters et al. (2018) measured only minor driver behavior adaptations to this additional optical flow. Third, the control loading of the steering wheel was manually tuned to better match the feel of a typical passenger car, resulting in a stiffness of 10 N m/rad (≈ 0.17 N m/deg); the rotational limit was increased relative to van der El et al. (2020), but for safety still limited to ±2 rad (≈ ±115 deg). All other experimental settings were equal to van der El et al. (2020), including the road trajectory, the external disturbances, and the vehicle's constant forward velocity (50 km/h).

3.4. Participants, instructions, and procedure

Eleven motivated volunteers participated, of which three did not finish due to emerging signs of motion sickness. The remaining eight participants (five male, three female) were on average 26.4 years old ($\sigma = 2.8$ years), were in possession of a driver's license for 5 years ($\sigma = 2.2$ years), and drove 7,400 km/year ($\sigma = 6{,}000$ km). All participants signed for informed consent before starting the experiment. Participants were instructed to drive as they would normally do in the lane-keeping tasks, and to minimize the lateral position error relative to the centerline in the tracking tasks.

Participants started with a five-run training phase, to familiarize themselves with the simulator and the given driving task. The LK-PR task was first performed with the wind-gust disturbances switched off, such that participants had a good feel for how their steering changed the vehicle's heading and lateral position before the disturbances were switched on in the second run. Subsequently, the LK-FG, TR-PR, and TR-FG tasks were practiced. These training data were not further analyzed.

Then, the measurement phase of the experiment commenced. The four experimental conditions were performed in an order randomized according to a balanced Latin-square design. A condition was performed at least until the average deviations from the centerline and steering wheel deflections were approximately constant in five consecutive runs, indicating that the participant's initial learning and adaptation curve had flattened. After each run, participants were given a performance score to motivate them, defined as the root-mean-square of the car deviations from the centerline in tracking tasks, and as cumulative road departures in lane keeping tasks. They were additionally asked to indicate signs of emerging motion sickness on the 11-point MIsery SCale (MISC, Bos et al., 2005); for comfort of the participants, the experiment was directly terminated when a MISC score of 5 or higher (first onset of nausea) was given. To reduce fatigue, participants left the simulator after each condition for a 10-20 min break, before moving on to the next condition. The experiment was typically completed in three hours.

3.5. Dependent measures

Two categories of dependent measures were calculated from the data. Those that could be directly obtained from the data (nonparametric measures) and those that required fits of the driver model. All measures presented in this paper are explained below in order of occurrence. Various more control-theoretic measures that were computed from the experiment data can be found in van der El (2018), including spectral densities, crossover frequencies and phase margins.

3.5.1. Nonparametric measures

Position in the lane: Lateral position on the road was used as a measure of performance, and is characterized by the vehicle's deviation y_e from the centerline. The standard deviation σ_{y_e} is used to compare driving performance to literature (Allen et al., 1975, Allen & O'Hanlon, 1979, Land & Horwood, 1998, Hildreth et al., 2000, Mars, 2008, Lakerveld et al., 2016, Wolters et al., 2018). The contributions due to the external target $y_c(t)$, lateral position disturbance $y_d(t)$, and heading disturbance $\psi_d(t)$ signals, as well as due to the human remnant $n(t)$ (remaining frequencies), are characterized by the standard deviation σ_{y_e} at each respective set of input frequencies, that is, ω_{y_c}, ω_{y_d}, ω_{ψ_d}, and ω_n. These separate contributions were calculated in the frequency domain, following the methodology detailed in van der El, Pool, et al. (2018), van der El, Padmos, et al. (2018). To better show the variability between conditions, all 95% confidence interval errorbars shown in our results figures were corrected for between-participant variability, by adjusting the means of individual participants' data to the overall grand mean of the data. The target-to-error dynamics $Y_e(j\omega)/Y_c(j\omega)$ were estimated to further quantify road-following performance, see van der El, Pool, van Paassen, et al. (2019) for details.

Lateral acceleration: The standard deviation (SD) of the lateral vehicle acceleration σ_{a_y} was used to compare the performed driving task with measurements obtained in the real world and other simulator driving tasks (Reymond et al., 2001, Xu et al., 2015).

Intermittent control behavior: The level of intermittent control was characterized by the time $T_{\dot{\delta}\approx 0}$ for which participants have an approximately constant control input. To estimate $T_{\dot{\delta}\approx 0}$, the control input was assumed to be constant when the steering wheel deflection rate $\dot{\delta} < 3$ deg/s, identical to Godthelp (1986), but only for periods longer than 0.3 s to omit steering reversals. The time to line crossing (TLC) was used as measure for the incentive for continuous control, opposed to intermittent control (Godthelp, 1986). The TLC indicates the time before any side of the vehicle will hit a lane edge, when the current steering wheel angle is maintained, see Fig. 1. The *curved* TLC was calculated, by extrapolating both the current heading angle and rate, see Godthelp (1986), Boer

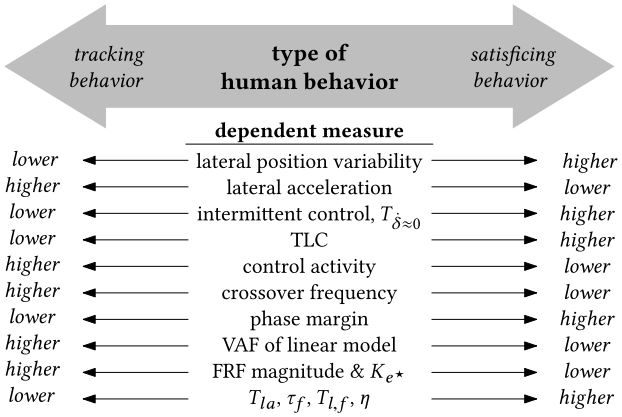

Fig. 4. Hypothesized qualitative changes in the dependent measures when driver behavior shifts between pure tracking and satisficing control.

(2016) for details. The alternative *straight* TLC was not considered, because neglecting the heading rate would yield a poor estimate of the actual time until road departure, due to the considerable road curvatures used in this experiment. The vehicle was assumed to be 1.5 m wide, identical to Boer (2016). For the tracking tasks a 'virtual TLC' was calculated for comparison with the lane-keeping tasks, by assuming the same road width (3.5 m).

Control activity: The SD of the steering wheel position σ_δ was used as measure for control activity. Identical as is done for the lateral position, σ_δ was further separated into contributions due to the target and disturbance signals and the human remnant.

3.5.2. Driver modeling-related measures

Estimates of the human's multiloop control dynamics were used as an explicit measure for driver visual cue selection, information processing, and control behavior. These measures include multiloop Frequency-Response Function (FRF) estimates ($H_{o_{y_c}}(j\omega)$, $H_{o_y}(j\omega)$, and $H_{o_\psi}(j\omega)$), estimates of the parameters of the multiloop driver model ($K_{e\star}$, $T_{L,e\star}$, τ_v, ω_{nms}, ζ_{nms}, T_{la}, τ_f, and $T_{l,f}$), and the estimated visual angle η that is minimized through compensatory control. For the model parameter estimates, the multiloop driver model is first fit to the data, before the look-ahead time $T_{la} = 1/(U_0 K_y^\psi)$ is computed from the estimated value of K_y^ψ in a second step (van der El et al., 2020). Fig. 1 illustrates the physical meaning of the model look-ahead times and the visual angle η.

To quantify human adaptation in even more detail than in van der El et al. (2020), a second-order model for the human's neuromuscular system (NMS) actuation dynamics (identical as in van der El, Pool, et al. (2018), van der El, Padmos, et al. (2018)) is also included in the compensatory control response $H_o^{comp}(j\omega)$. Corresponding to Fig. 2, the modeled control output as a function of the optical angle η is then given by $\hat{\delta}(j\omega) = H_o^{comp}(j\omega)\eta(j\omega) + N(j\omega)$, with remnant N and:

$$H_o^{comp}(j\omega) = K_{e\star}(1 + T_{L,e\star} j\omega)e^{-\tau_v j\omega} \frac{\omega_{nms}^2}{(j\omega)^2 + 2\zeta_{nms}\omega_{nms} j\omega + \omega_{nms}^2} \tag{1}$$

In Eq. (1), ω_{nms} and ζ_{nms} are the neuromuscular break frequency and damping ratio, respectively. To avoid obtaining physically unrealistic break frequencies and damping ratios, constraints of $\omega_{nms} < 18$ rad/s and $0.05 < \zeta_{nms} < 0.4$ were applied while estimating the parameters from the data.

Note that the modeled delay τ_v represents *only* the human's visual response delay, as opposed to the original model from van der El et al. (2020), where the delay captured both the human's visual response delay *and* the phase effects of the NMS.

3.6. Hypotheses

H.I Restricted preview affects human control behavior identically as in single-loop tracking tasks (van der El, Padmos, et al., 2018). An expected main effect is larger lateral position variations in the lane (higher σ_{y_e}). In terms of the driver model, these are caused by limiting the most distant visual trajectory input to the driver (τ_f) to 0.5 s ahead, and, as $\tau_f = T_{la} + T_{l,f}$, this limits the driver's ability to anticipate (T_{la}) and smooth ($T_{l,f}$) the trajectory's curves.

H.II Drivers are hypothesized to show higher levels of satisficing control behavior in lane-keeping tasks (LK) with full preview, as compared to centerline-tracking (TR) tasks, but *not* when preview is restricted. There is thus an interaction effect of road presentation and restricted preview on driver steering behavior. While available lane width increases the range of acceptable vehicle trajectories, it is expected that drivers can exploit this additional freedom *only* when there is adequate baseline performance and stability, which may not be attained when fog limits the preview of the road ahead. Fig. 4 illustrates the changes in the dependent measures that are expected to occur when participants show higher levels of satisficing control behavior in LK-PR tasks.

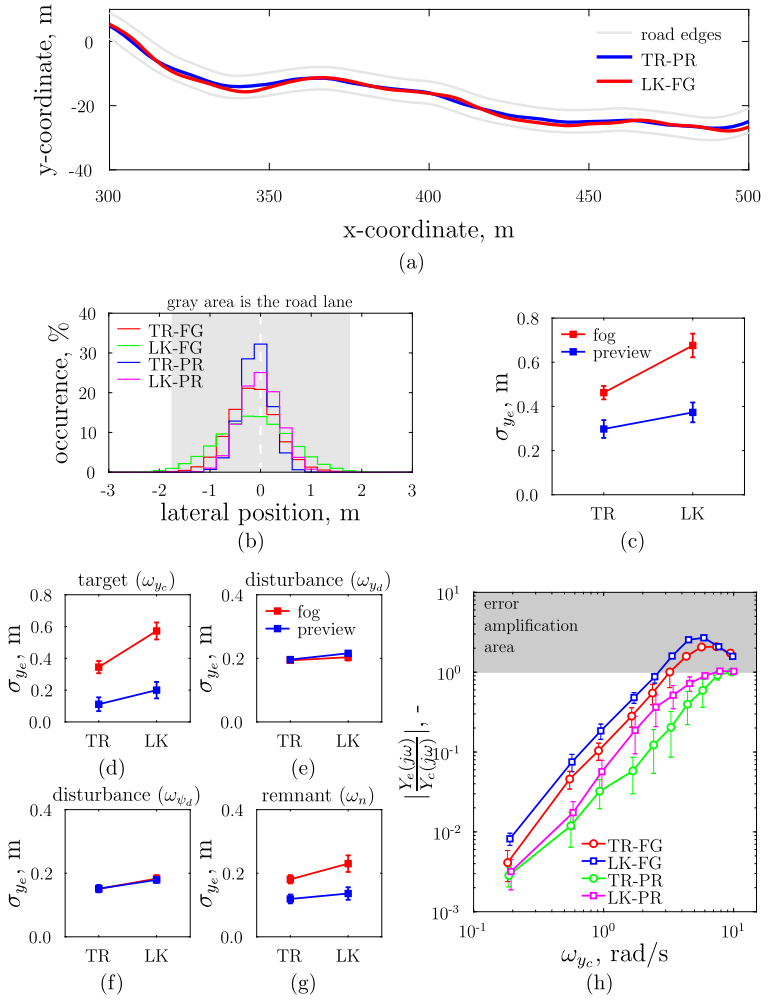

Fig. 5. Lateral position deviations y_e from the road centerline: a top view of representative traveled paths in single runs of LK-FG and TR-PR tasks (a); the y_e distribution summed over all eight participants (b); the average standard deviations of y_e of the eight participants (c-g), with 95% confidence intervals (corrected for between-participant variability); and the target-to-error dynamics, average of eight participants and standard deviations (h). (For interpretation of the colors in the figure(s), the reader is referred to the web version of this article.)

4. Results

4.1. Nonparametric measures

4.1.1. Position on the road

Fig. 5a shows a portion of the road, together with the trajectories traveled by a representative participant in the conditions where the average lateral deviations were found to be the largest (LK-FG) and smallest (TR-PR). The vehicle trajectories both follow the road trajectory, but the absence of preview in the LK-FG task clearly results in vehicle trajectories that are often closer to the road edges. This is confirmed by the lateral position distributions on the road (Fig. 5b), which show that the vehicle's center of gravity seldomly crosses the road's boundaries, except occasionally in the LK-FG condition. Figs. 5b and 5c both show that participants keep their vehicle closer to the road's centerline in TR tasks (opposed to LK), and when preview is available (opposed to FG). In the nominal driving task (LK-PR), σ_{y_e} is on average 0.38 m, which is higher than typical deviations ($0.1 < \sigma_{y_e} < 0.3$ m) reported throughout literature (Allen et al., 1975, Allen & O'Hanlon, 1979, Land & Horwood, 1998, Hildreth et al., 2000, Mars, 2008, Lakerveld et al., 2016). Yet, the measured performance is comparable to the similar simulator experiment by Wolters et al. (2018), which also included relatively strong external disturbances.

Figs. 5d–5g show that the target y_c, disturbances y_d and ψ_d, and remnant n all contribute to the increase in total y_e between TR and LK tasks, but that the increase is largest at the input frequencies of the target signal (i.e., the road trajectory). Restricted preview mainly results in poorer target tracking, very similar as in single-loop tracking tasks (see van der El, Padmos, et al., 2018), by inhibiting participants from anticipating the road's upcoming curves. Disturbance rejection is only marginally affected by restricted preview, both in TR (corresponding to van der El, Padmos, et al., 2018) and LK tasks. Lateral position deviations at remnant

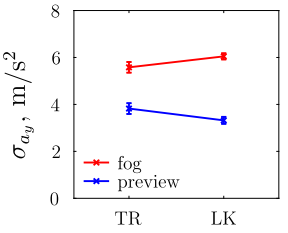

Fig. 6. Standard deviation of the vehicle lateral accelerations a_y; average of eight participants and 95% confidence intervals, corrected for between-subject variability.

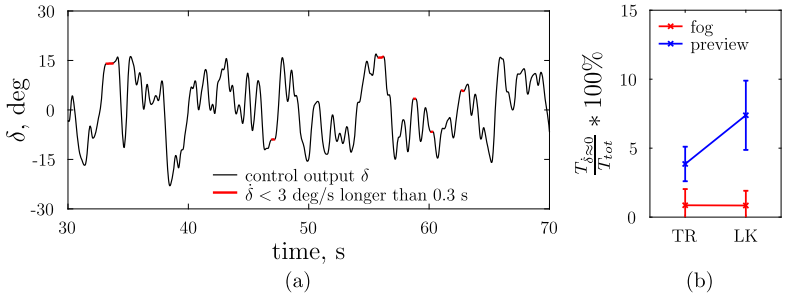

Fig. 7. Time that the control output is approximately constant, single-run data of a representative participant in the LK-PR condition (a) and the average of eight participants (b), with 95% confidence intervals (corrected for between-participant variability).

(n) frequencies increase for FG compared to PR tasks, see Fig. 5g, indicating an increase in nonlinear, time-varying behavior, or perception or motor noise.

The measured target-to-error dynamics are shown in Fig. 5h. In PR tasks, the magnitude of the target-to-error dynamics is always smaller than unity, which indicates that drivers could track all frequency components of the trajectory ahead, albeit less accurately for the higher-frequency components. In contrast, in FG tasks the magnitude is larger than unity at frequencies above 2.5 rad/s, indicating that here the participants' steering efforts *increased* the vehicle's deviation from the centerline as compared to a 'no-control' strategy (do nothing). Such error amplification results from the human's visual response time delay when performing closed-loop feedback control, and reflects the 'jerky' control behavior that is reported in driving experiments were the 'far visual field' is occluded (Land & Horwood, 1995a, Frissen & Mars, 2014, Mole et al., 2016). Identical to the single-loop tracking tasks in (van der El, Pool, et al., 2018, van der El, Pool, van Paassen, et al., 2019), preview allows participants to anticipate the target trajectory to compensate for their own response lags, which, consequently, eliminates the amplification peak.

4.1.2. Lateral acceleration

The standard deviations of the vehicle lateral accelerations σ_{a_y} are on average between 3 and 6.5 m/s^2, see Fig. 6. The lateral acceleration is 50-100% higher when preview is restricted (compared to PR tasks). Opposed to TR, LK yields lower accelerations when preview is available, but higher accelerations when preview is limited.

The measured lateral accelerations in the nominal driving task (LK-PR) are in general below 11 m/s^2 ($= 3\sigma_{a_y}$, 99.7% of the sampled data). This is markedly higher than the maximum $a_y \approx 5$ m/s^2 reported for real-world driving scenarios in Xu et al. (2015), and also higher than the peak of around 9 m/s^2 in other simulator driving experiments (e.g., in Reymond et al., 2001). The high accelerations are a direct result of the fixed forward vehicle velocity, the strong lateral wind-gust disturbances (y_d and ψ_d), and relatively high road curvatures ($\sigma = 0.0175$ m^{-1}). Moreover, the performed experiment lacked physical motion feedback, the absence of which is known to lead to more aggressive control behavior (Wolters et al., 2018), and higher lateral accelerations (Reymond et al., 2001).

4.1.3. Intermittent control

Fig. 7 shows the time $T_{\dot{\delta}\approx 0}$ for which participants kept the steering wheel angle δ constant, the *intermittent* control output. Overall, Fig. 7 shows that participants seldomly kept their control output δ constant for a sustained period of time. Especially when preview is restricted by fog, $T_{\dot{\delta}\approx 0}$ approaches zero, indicating continuous closed-loop control activity. With preview, $T_{\dot{\delta}\approx 0}$ is clearly higher and increases further from TR to LK tasks. However, even in LK-PR tasks, the average time that participants kept the steering wheel angle approximately constant is below 10% of the total measurement time (Fig. 7b). Although no comparable results are available from literature, the $T_{\dot{\delta}\approx 0}$ values are likely relatively low due to the characteristics of the performed driving task, with its constantly varying road curvature and persistent quasi-random external disturbances (ψ_d and y_d).

4.1.4. Time to line crossing

The TLC was on average between 0.5 and 1.5 s throughout the experiment, see Fig. 8. This is lower than what is typically observed in curve driving tasks (e.g., TLC > 3 s (Godthelp, 1986)), which is a direct result of the road's constantly varying curvature, as well as the high average curvature, in combination with the vehicle's fixed velocity. Availability of preview leads to a notably higher TLC

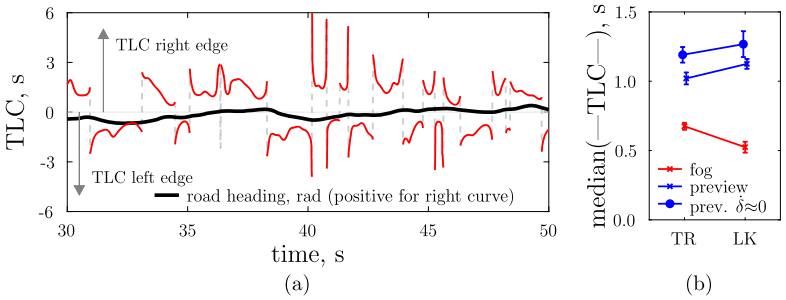

Fig. 8. The curved TLC, single-run data of a representative participant in the LK-PR condition (a), and the median of eight participants (b), with 95% confidence intervals (corrected for between-participant variability); in tracking, TLC is based on a virtual 3.5 m wide road.

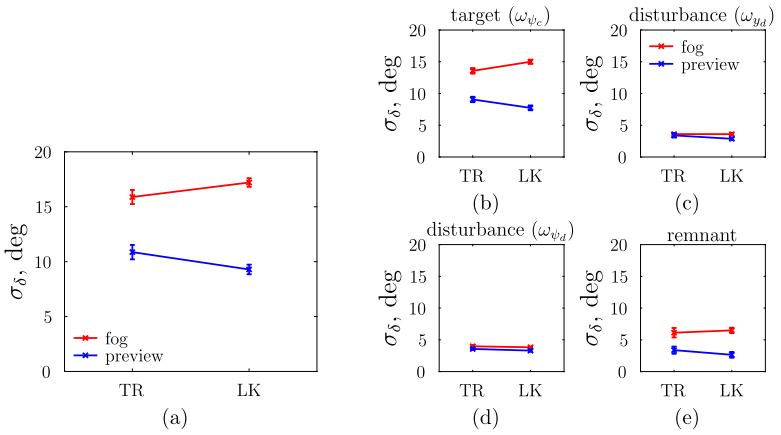

Fig. 9. Standard deviations of the control output δ (a-e), average of eight participants and 95% confidence intervals (corrected for between-participant variability).

(Fig. 8b). Compared to the 'virtual' TLC in tracking tasks, lane-keeping yields a higher TLC in preview tasks, but a lower TLC in tasks with fog, suggesting that available lane width makes the task more difficult without preview and easier with preview.

For the conditions with preview, during the periods where the control output is constant (Fig. 7), the TLC is around 0.2 s higher than the average TLC measured throughout the full experiment (see the "x" markers in Fig. 8b). Higher TLCs thus indeed appear to evoke less steering corrections, as suggested previously by Godthelp (1986).

4.1.5. Driver steering wheel activity

The standard deviation of the control activity σ_δ, shown in Fig. 9a, is 50-75% higher in tasks with fog (compared to PR). This contradicts single-loop tracking results from van der El, Pool, et al. (2018), where identical control activity was measured in tasks with and without preview. From TR to LK tasks, participants increase their control activity σ_δ by approximately 10% without preview, but decrease σ_δ by around 20% with full preview. Lane keeping thus evokes less control activity than tracking in PR tasks, supporting the obtained TLCs that the LK task is easier and that the higher lateral position variability on the road (Fig. 5) is the result of *satisficing* control behavior.

In contrast, the higher lateral position variability in LK-FG tasks (compared to TR-FG) does *not* reflect satisficing behavior, as the accompanying higher control activity suggests that the task is *more difficult*. The increased task difficulty likely results from the visual presentation: comparing Figs. 3a and 3b shows that the centerline in TR tasks is more salient than the lane edges in LK tasks. Note that changes in σ_δ between conditions are strongly correlated to the vehicle's lateral accelerations, compare Fig. 9a and Fig. 6.

Figs. 9b–9e show that the target frequencies account for over 50% of the total σ_δ, such that over 75% of the control output *power* (σ_δ^2) is primarily dedicated to *target tracking*. Neither of the independent variables has a marked effect on the control output power at the frequencies of the disturbance signals y_d (Fig. 9c) and ψ_d (Fig. 9d). Fig. 9e shows that the control activity at the remnant (n) frequencies increases for FG compared to PR tasks, which is mainly a consequence of the higher total control activity (Fig. 9a) with which remnant typically scales (Levison et al., 1969). The increased remnant activity explains why σ_{y_e} at the remnant frequencies was also higher in FG tasks, see Fig. 5g.

4.1.6. Driver frequency response function (FRF)

FRF estimates of driver multiloop control dynamics are given by markers in the Bode plots in Figs. 10 and 11. The shapes of the three measured FRFs are identical in TR and LK tasks, both with and without preview, which indicates that participants adopt a

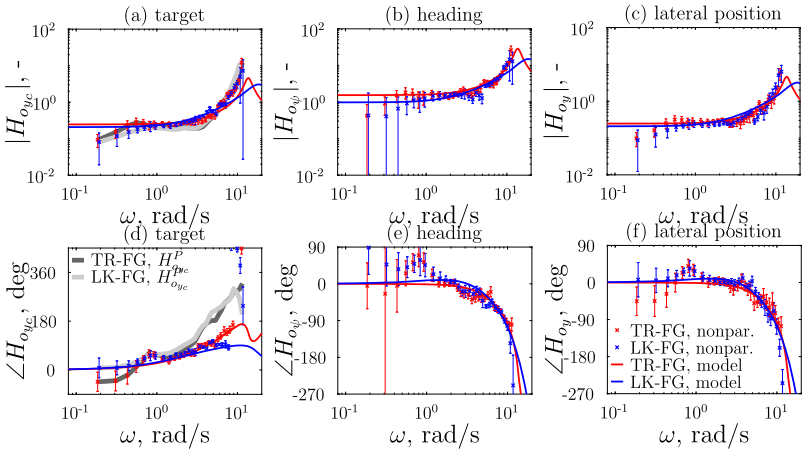

Fig. 10. Bode plots of the multiloop steering dynamics of a representative participant in conditions with fog (TR-FG and LK-FG): nonparamteric FRF estimates with standard errors, perfect target-tracking dynamics, and the model fits.

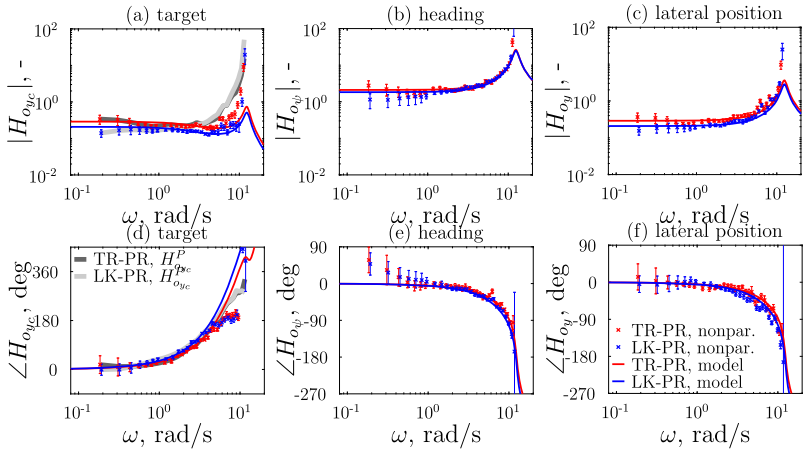

Fig. 11. Bode plots of the multiloop steering dynamics of a representative participant in conditions with full preview (TR-PR and LK-PR): nonparametric FRF estimates with standard errors, perfect target-tracking dynamics, and the model fits.

similar control strategy. Restricted preview has some notable effects, in particular on the target feedforward response $H_{o_{y_c}}(j\omega)$, as is well-known from tracking tasks (van der El, Padmos, et al., 2018). With fog, less phase lead and a higher FRF magnitude is visible at the higher input frequencies of $H_{o_{y_c}}(j\omega)$, indicating less centerline trajectory anticipation and smoothing, respectively. Participants adopt a target response $H_{o_{y_c}}(j\omega)$ that approximates the $H^P_{o_{y_c}}(j\omega)$ dynamics required for *perfect* target-tracking, see van der El et al. (2020); however, they mainly match the *phase* of $H^P_{o_{y_c}}(j\omega)$ in preview tasks and its *magnitude* in tasks with restricted preview, indicating that synchronizing the vehicle with the centerline oscillations is prioritized in PR tasks. These effects correspond to the experimental results in van der El, Padmos, et al. (2018), where available preview was limited in single-loop tracking tasks.

4.2. Driver model-related results

4.2.1. Model quality-of-fit

The dynamics of the fitted multiloop driver model are also shown in Figs. 10 and 11, together with the estimated FRFs. In general, the driver model captures the shape of all three FRF estimates well in all four tasks, with the following exceptions:

- The highest frequencies of the feedforward response $H_{o_{y_c}}(j\omega)$, Figs. 10 and 11 (a,d), especially in preview tasks, because participants ignore the highest frequencies of the target trajectory, see Fig. 9.
- The lowest frequencies of the heading response $H_{o_\psi}(j\omega)$, Figs. 10 and 11 (b,e), because, here, control output is dominated by the lateral position loop (Allen, 1981).

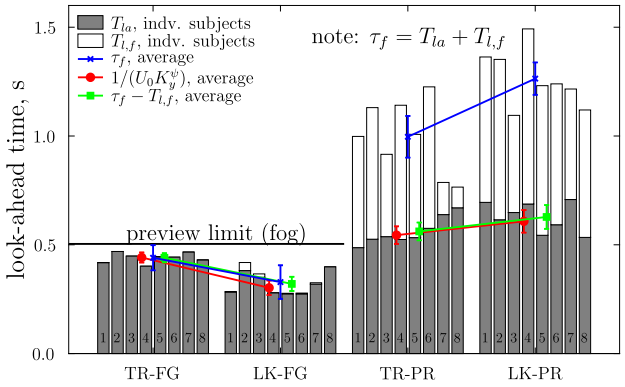

Fig. 12. Estimated feedforward anticipatory control behavior parameters; individual participants are shown with bars, markers indicate the average and 95% confidence intervals (corrected for between-participant variability). White bars are hardly visible in tasks with fog, as $T_{l,f}$ is approximately zero for most participants. The feedback and feedforward look-ahead time parameters, $1/(U_0 K_y^{\psi})$ and $\tau_f - T_{l,f}$, respectively, which correspond to T_{la}, are shown for comparison with van der El et al. (2020).

- The highest frequencies of all three FRFs in the LK-FG task; here, the neuromuscular system dynamics were difficult to estimate, likely because the break frequency ω_{nms} is beyond the highest forcing function input frequency (11.5 rad/s).

In addition to capturing the estimated FRFs of participants' multiloop steering dynamics, the model also accurately matches participants' steering outputs, as model VAFs are high (>95% for all participants in all experimental conditions). In fact, even when considering the measured control outputs (δ) in a single run – opposed to the five-run average considered throughout this paper – the human's control output is accurately captured. Together, these results indicate that the unified driver model proposed in van der El et al. (2020) not only captures driver behavior in centerline-tracking tasks with full preview (TR-PR), but can also be applied in more realistic lane-keeping tasks, including situations with limited visibility. This considerably extends the applicability of the quasi-linear driver modeling framework.

4.2.2. Anticipatory control behavior

The estimated feedforward model parameters T_{la}, $T_{l,f}$, and τ_f are shown in Fig. 12. In tasks where preview was restricted by fog, the farthest point of the centerline trajectory ahead that is used by participants, characterized by τ_f, is well within the remaining 0.5 s visible region ahead of the vehicle. Note that τ_f was not constrained during identification and was free to take any value. This supports that the quasi-linear model's look-ahead times have physical meaning and can be interpreted as such, and reflect the portion of the previewed trajectory used by drivers for control (see Fig. 1), identical as in single-loop preview tracking tasks (see Rezunenko et al., 2018, van der El, Padmos, et al., 2018). In fact, in TR-FG and LK-FG tasks, the most distant target point used for control (τ_f) lies 0.44 s and 0.33 s ahead of the vehicle, respectively, such that *not all* the 0.5 s of available preview information is exploited. This is likely the consequence of the poor contrast of the road trajectory at the 0.5 s limit where it disappears in the fog (see Fig. 3). Because in our experiment the white centerline in TR tasks is easier to perceive up to the preview limit (thicker line, brighter white) than the road lane edges in LK tasks, participants can adopt a larger look-ahead time. This explains exactly why the LK-FG task was more difficult than the TR-FG task, as suggested before by the lateral position deviations (Fig. 5), the TLCs (Fig. 8) and the control activity (Fig. 9a): the experiment's visual scene made it more difficult for participants to use the full 0.5 s of 'theoretically' available preview.

Fig. 12 further shows that restricted preview severely limits participants to both anticipate (T_{la}) and smooth ($T_{l,f}$) the target trajectory. The most distant point on the trajectory ahead that is used for control (τ_f) decreases substantially, from around 1.2 s in tasks with preview to around 0.4 s in tasks with fog. Interestingly, participants do not smooth the target trajectory at all in tasks with fog ($T_{l,f} \approx 0$ s) and use all of the remaining preview for anticipation (T_{la}), that is, to compensate for vehicle lag and their own response delay. The look-ahead time T_{la} is decreased only slightly when preview is restricted, from around 0.6 (PR) to 0.4 s (FG) ahead. A lower T_{la} implies that participants rely relatively more on lateral position feedback and less on heading feedback (as explained in van der El et al., 2020 and Weir & McRuer, 1970, McRuer et al., 1975, Allen, 1981), which corresponds with the fact that the (still visible) 'near visual field' provides mostly lateral position information (Grunwald & Merhav, 1976, Land & Horwood, 1995a). In tasks with preview, lane-keeping (LK-PR) leads to more trajectory smoothing than centerline tracking (TR-PR): $T_{l,f}$ on average increases from 0.43 to 0.64 s. This indicates that the higher-frequency oscillations of the road trajectory are ignored.

4.2.3. Feedback control behavior

As explained in detail in (van der El et al., 2020), the model fits yield two independent estimates of the look-ahead time T_{la}, namely $1/(U_0 K_y^{\psi})$ for the feedback responses and $\tau_f - T_{l,f}$ for the feedforward response. Fig. 12 shows that these two T_{la} estimates are almost identical also in the more realistic tasks tested here, supporting the key finding of van der El et al. (2020). The main implication of this fact is the model suggests that drivers minimize the visual angle η between the vehicle's heading and a 'target' heading, obtained by smoothing a portion of the centerline trajectory. Recall that Fig. 1 illustrated this visual angle, which was

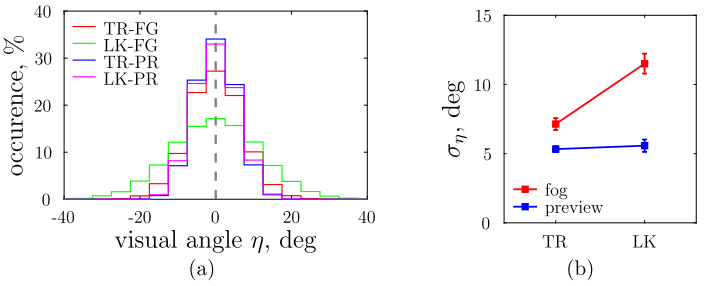

Fig. 13. The visual angle η that drivers minimize through compensatory control.

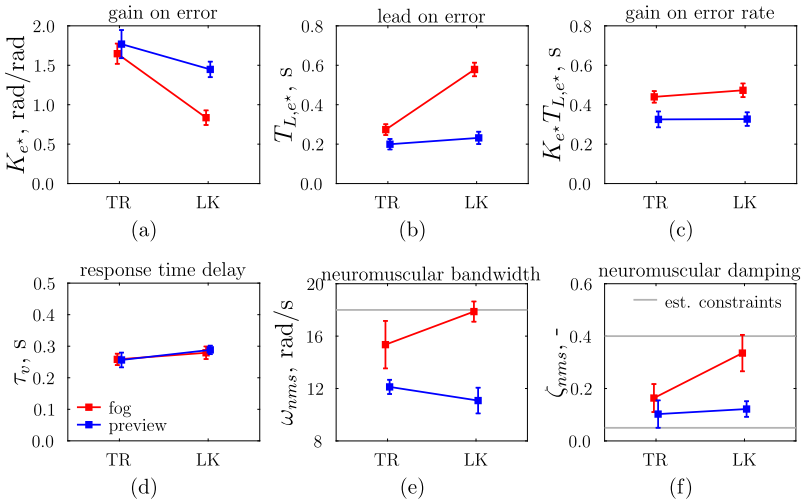

Fig. 14. Estimated compensatory response parameters; average of eight participants and 95% confidence intervals (corrected for between-participant variability). Gray lines indicate the parameters estimation constraints imposed on ω_{nms} and ζ_{nms}.

drawn for a look-ahead time that corresponds to the measured LK-PR task data: $T_{la} = 0.6$ s and $\tau_f = 1.25$ s. This self-generated η is the signal that is minimized by drivers through compensatory feedback control, see also van der El et al. (2020). Using the estimated look-ahead times in open-loop model simulations, the actual visual angles η could be estimated, the results of which are shown in Fig. 13. The visual angle η is generally below ±20 deg, so the target heading or 'aim point' (T_{la} s ahead) is always well within the driver's visual field when he or she looks straight ahead. The magnitude of the visual angle increases in tasks where the deviations from the centerline are larger (Fig. 5), leading to the largest angles in LK-FG tasks and the smallest angles in TR-PR tasks.

Fig. 14 shows the estimated parameters of the compensatory submodel, which quantify how participants minimized the visual angle η. Compared to TR tasks, participants reduce their gain $K_{e\star}$ in LK tasks, that is, they minimize η less aggressively. In tasks with restricted preview, in particular in lane-keeping tasks (LK-FG), participants generate more lead ($T_{l,e\star}$). The fog limits the heading information conveyed by the visual scene, leading to a lower T_{la} and reduced stability (see van der El et al., 2020), which must then be compensated for by a stronger reliance on *predictive* behavior (higher $T_{L,e^\star}$). Participants have a slightly higher visual delay τ_v during LK as compared to TR tasks.

Tentatively, the 'error' directly visible in the tracking task motivates participants to put additional effort into reducing their response delay to increase performance. An identical increase in response delay was observed when additional heading feedback was made available in single-axis preview tracking tasks (van der El et al., 2020). Finally, participants also markedly adapt their neuromuscular system dynamics to the task. The NMS break frequency ω_{nms} trends resemble those found for control activity, Fig. 9a. The NMS break frequency increases from lane-keeping to centerline-tracking tasks with preview from 9.5 (LK-PR) to 12 rad/s (TR-PR); then to 15.5 rad/s when preview is restricted in tracking tasks (TR-FG), and finally to 18 rad/s in lane-keeping tasks with fog (LK-FG), where the highest control activity is observed.

5. Discussion

It was hypothesized (H.I) that in a (more) realistic driving task, limiting the preview ahead would affect human control behavior identically as in classical single-loop preview tracking tasks (van der El, Padmos, et al., 2018). Indeed, fog led to increased lateral position deviations from the road's centerline. Disturbance-rejection was barely affected by limited visibility. Model fits showed that drivers' main steering adaptation is to use road preview information from less far ahead, below the restricted preview limit of 0.5 s, opposed to using approximately 1.2 s in tasks with unrestricted preview. Limiting the available preview inhibits drivers from

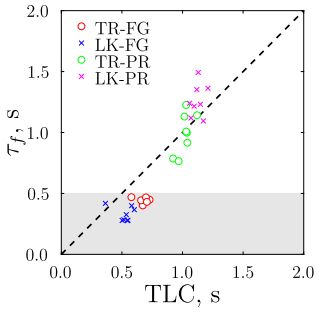

Fig. 15. Correlation between the TLC and the estimated farthest preview point used for control (τ_f); gray area indicates the available preview in tasks with fog (FG).

smoothing the road's trajectory; the remaining preview is instead used for anticipation. Without smoothing, the to-be-minimized self-generated visual angle η contains more high-frequency components, leading to higher control activity and higher lateral accelerations. With fog, drivers still select an aim point for the visual angle that is positioned as far ahead as possible, so the look-ahead time T_{la} is right below the 0.5 s preview limit, to maximize feedback performance for disturbance-rejection. These results support the first hypothesis (H.I).

The control-theoretic driver model from van der El et al. (2020) captures the measured driver steering behavior very well, including driver adaptation of their multiloop steering dynamics between the full and restricted preview cases. The preview time-related model parameters obtained from fitting the model to the three frequency response functions perfectly reflect the imposed viewing limitations (i.e., our restricted and unrestricted preview cases), revealing that in our experiment the drivers always used the complete visual preview available to them. The self-generated visual angle η was reconstructed to be below ± 20 degrees, which means that the aim-point generally lies in front of the vehicle, but with preview available considerably smoothed relative to the future trajectory. While it can be expected that drivers outside our limited test pool of eight participants will achieve both higher and lower performance, control activity, and TLCs, the observed low-level loop closures and control adaptations to limited preview (fog) and road boundaries seem generalizable.

We also hypothesized (H.II) that drivers show higher levels of satisficing control behavior in lane-keeping tasks (LK) as compared to centerline-tracking tasks (TR), but only with full preview. This hypothesis is also confirmed, as all dependent measures reflect a higher level of satisficing control in LK tasks with preview, as compared to TR, see Fig. 4. In particular, the lateral deviation from the lane centerline, the TLC, and the intermittent steering wheel control ($T_{\delta \approx 0}$) all increase, while drivers steer less aggressively (lower $K_{e^\star}$), minimize the visual angle farther ahead (higher T_{la}) and ignore more of the road trajectory's higher frequencies (higher $T_{l,f}$). With limited preview, lateral deviations also increase from TR to LK tasks; however, this is not a manifestation of more satisficing behavior per se, but rather the result of the smaller look-ahead time, as a consequence of the limited visual contrast between the rendered lane edges and the simulated fog in LK-FG tasks.

In our experiment, differences in driver behavior between tracking en lane-keeping tasks are smaller than expected, and no clear, discrete control-mode 'switch' was observed from tracking to satisficing behavior. Instead, the switch to more satisficing and less tracking control appears to be gradual, as graphically indicated in Fig. 4 and as suggested by Gray (2005, 2008). The relative level of satisficing or tracking behavior in a driving task likely depends on driver experience and task difficulty, characterized by variables such as the vehicle dynamics, road curvature and lane width, and the presence and strength of external (wind-gust) disturbances. The low TLC values in our experiment suggest that participants exhibited only limited levels of satisficing control behavior. Experiments with more realistic road-curvature profiles and less strong external disturbances likely result in higher TLCs, and may, consequently, evoke more pronounced satisficing behavior. Such future experiments are a key next step for further extending the applicability of the proposed quasi-linear model to explain driver steering in more realistic driving tasks. However, the lower power of the road and disturbance signals will excite the driver dynamics less, inevitably leading to less accurate driver modeling data.

The TLC is often considered as a measure for drivers' incentive to steer: when the TLC drops below a certain threshold, steering corrections are required to avoid lane departures. Estimated control-theoretic model parameters in our experiment suggest that participants respond to the road trajectory τ_f s ahead, such that there may be a correlation with the TLC. Fig. 15 shows that a correlation between the experimental TLCs and the model's look-ahead times τ_f indeed appears to exist, especially in tasks with full preview. More experimental data are needed to verify whether such a relation holds over a wide range of task variables. Larger TLCs in general occur in less demanding driving tasks (Godthelp et al., 1984, Godthelp, 1986). Correspondingly, here, less demanding tasks also lead to higher model look-ahead times, as is visible, for example, from the difference between TR-PR and LK-PR in Fig. 12.

Like many earlier investigations into driver steering (Land & Horwood, 1995b, Land & Lee, 1994, Weir & McRuer, 1973, van der El et al., 2020, Wolters et al., 2018, McRuer et al., 1975, McLean & Hoffmann, 1972, McRuer et al., 1977, Lakerveld et al., 2016), in our experiment the driving speed was kept constant (here at 50 km/h) to collect 'clean' data on how drivers steer through curves. In reality, drivers are of course known to reduce their vehicle's speed before an approaching tight curve (van Winsum & Godthelp, 1996, Bella et al., 2014) and in restricted viewing conditions (van der Hulst et al., 1998, Broughton et al., 2007, Caro et al., 2009, Yan et al., 2014, Li et al., 2015, Siebert & Wallis, 2019, Huang et al., 2020, Zolali & Mirbaha, 2020) to reduce risk, lower experienced lateral accelerations, and improve steering precision. As such speed reductions are thus a key characteristic of how drivers steer through curves, we intent to measure and include driver adaptation to driving speed into the proposed model as the next step in

our research. It will be essential to compare steering adaptations between various fixed driving speeds with self-imposed, continuous speed changes. For the latter, a time- or parameter-varying modeling approach may prove unavoidable. How drivers exactly adapt their *steering* behavior as a function of driving speed is still poorly understood today.

With an accurate fit to measured steering data in the frequency domain and intuitively interpretable parameters, the proposed driver modeling method provided new insight into steering behavior variations across a wide range of viewing conditions. We foresee that the same approach can be followed to extend our modeling framework to include variable speed. First, the current experiment setup can be used to measure how drivers steer at different (constant) driving speeds, which will show how key steering parameters (e.g., T_{la} and $T_{l,f}$) vary with speed. Then, these *steady-state* differences in steering behavior can be directly compared to steering behavior in "normal" speed-varying tasks, to obtain a time- or parameter-varying driver model (Godthelp et al., 1984, MacAdam, 2003, Mulder et al., 2018). This is the crucial next step for driver steering modeling towards its key real-world applications, such as the development of more 'human-like' lane-keeping assist systems and other steering ADAS.

6. Conclusion

Experimental data are presented to investigate, and to model, differences between driver steering behavior in centerline-tracking and lane-keeping tasks, with full or restricted preview. When preview is restricted, drivers use as much as possible of the remaining preview to anticipate the curves of the road ahead, but cease to use preview for 'smoothing' the trajectory (a phenomenon known as 'corner cutting'). Steering behavior measured in the experiment mostly resembles tracking and *not* satisficing control, both in tracking *and* lane-keeping tasks, as near-continuous steering was required to follow the constantly-varying road curvature and suppress the external disturbances. Traditional time-domain measures (steering angle, TLC) and estimated model parameters all point to emergent satisficing behavior in the lane-keeping, curve driving task with preview: drivers steer less aggressively, more intermittently, and ignore more of the road's fast changes, which leads to a larger lateral position variability within the lane. For the first time, these adaptations in driver multiloop steering dynamics with and without preview could be modeled, extending the quasi-linear driver modeling framework extensively. The model's physically interpretable parameters provide novel quantitative insights, in particular regarding how drivers adapt their use of the visual cues provided by the road ahead when visibility conditions change. The model can be used to make steering support systems behave more human-like, or even to tailor them to an individual's behavior.

CRediT authorship contribution statement

Kasper van der El: Conceptualization, Data curation, Formal analysis, Investigation, Methodology, Software, Visualization, Writing – original draft, Writing – review & editing. **Daan M. Pool:** Conceptualization, Methodology, Software, Supervision, Writing – review & editing. **Marinus M. van Paassen:** Conceptualization, Methodology, Software, Supervision, Writing – review & editing. **Max Mulder:** Conceptualization, Funding acquisition, Methodology, Resources, Supervision, Writing – original draft, Writing – review & editing.

Data availability

Data will be made available on request.

References

Allen, R. W. (1981). Stability analysis of automobile driver steering control. In *Proc. 17th ann. conf. on manual control* (pp. 597–609).

Allen, R. W., & O'Hanlon, J. F. (1979). Effects of roadway delineation and visibility conditions on driver steering performance. *Transportation Research Record*, *739*, 5–8.

Allen, R. W., Jex, H. R., McRuer, D. T., & DiMarco, R. J. (1975). Alcohol effects on driving behavior and performance in a car simulator. *IEEE Transactions on Systems, Man and Cybernetics*, *5*, 498–505.

Allen, R. W., McRuer, D. T., Hogge, J. R., Humes, R. W., Stein, A. C., O'Hanlon, J. F., Hennessy, R. T., Kelley, G. R., & Bailey, G. V. (1977). *Drivers' visibility requirements for roadway delineation, volume I: Effects of contrast and configuration on driver performance and behavior*. Technical Report FHWA-RD-77-165, Systems Technology, Inc.

Barendswaard, S., Pool, D. M., & Abbink, D. A. (2019). A method to assess individualized driver models: Descriptiveness, identifiability and realism. *Transportation Research Part F*, *61*, 16–29.

Bella, F., Calvi, A., & D'Amico, F. (2014). Analysis of driver speeds under night driving conditions using a driving simulator. *Journal of Safety Research*, *49*, 45–52.

Boer, E. R. (2016). Satisficing curve negotiation: Explaining drivers' situated lateral position variability. In *Proceedings of the 13th IFAC/IFIP/IFORS/IEA symposium on analysis, design and evaluation of man-machine systems* (pp. 183–188).

Bos, J. E., MacKinnon, S. N., & Patterson, A. (2005). Motion sickness symptoms in a ship motion simulator: Effects of inside, outside, and no view. *Aviation, Space, and Environmental Medicine*, *76*, 1111–1118. http://www.ncbi.nlm.nih.gov/pubmed/16370260.

Brooks, J. O., et al. (2011). Speed choice and driving performance in simulated foggy conditions. *Accident Analysis and Prevention*, *43*, 698–705.

Broughton, K. L. M., Switzer, F., & Scott, D. (2007). Car following decisions under three visibility conditions and two speeds tested with a driving simulator. *Accident Analysis and Prevention*, *39*, 106–116.

Caro, S., Cavallo, V., Marendaz, C., Boer, E. R., & Vienne, F. (2009). Can headway reduction in fog be explained by impaired perception of relative motion? *Human Factors*, *51*, 378–392.

Demir, M., & Cavusoglu, A. (2012). A new driver behavior model to create realistic urban traffic environment. *Transportation Research Part F*, *15*, 289–296.

Deng, C., Wu, C., Cao, S., & Lyu, N. (2019). Modeling the effect of limited sight distance through fog on car-following performance using QN-ACTR cognitive architecture. *Transportation Research Part F*, *65*, 643–654.

Donges, E. (1978). A two-level model of driver steering behavior. *Human Factors*, *20*, 691–707.

Frissen, I., & Mars, F. (2014). The effect of visual degradation on anticipatory and compensatory steering control. *The Quarterly Journal of Experimental Psychology*, *67*, 499–507. https://doi.org/10.1080/17470218.2013.819518.
Godthelp, H. (1986). Vehicle control during curve driving. *Human Factors*, *28*, 211–221.
Godthelp, H., Milgram, P., & Blaauw, G. J. (1984). The development of a time-related measure to describe driving strategy. *Human Factors*, *26*, 257–268. https://doi.org/10.1177/001872088402600302.
Gordon, D. A. (1965). Static and dynamic visual fields in human space perception. *Journal of the Optical Society of America*, *35*, 1296–1303.
Gordon, D. A. (1966a). Experimental isolation of drivers' visual input. *Public Roads*, *33*, 266–273.
Gordon, D. A. (1966b). Perceptual basis of vehicular guidance. *Public Roads*, *34*, 53–68.
Gray III, W. R. (2005). Boundary-avoidance tracking: A new pilot tracking model. In *Proc. AIAA atmospheric flight mechanics conference and exhibit* (pp. 1–12).
Gray III, W. R. (2008). A generalized handling qualities flight test technique utilizing boundary avoidance tracking. In *Proc. U.S. Air Force T&E days* (pp. 1–19).
Grunwald, A. J., & Merhav, S. J. (1976). Vehicular control by visual field cues – analytical model and experimental validation. *IEEE Transactions on Systems, Man and Cybernetics*, *6*, 835–845. https://doi.org/10.1109/TSMC.1976.4309480.
Hess, R. A., & Modjtahedzadeh, A. (1989). A preview control model of driver steering behavior. In *Proc. of the IEEE conference on systems, man, and cybernetics* (pp. 504–509).
Hildreth, E. C., Beusmans, J. M. H., Boer, E. R., & Royden, C. S. (2000). From vision to action: Experiments and models of steering control during driving. *Journal of Experimental Psychology. Human Perception and Performance*, *26*, 1106–1132. https://doi.org/10.1037//0096-1523.26.3.1106.
Huang, Y., Yan, X., Li, X., & Yang, J. (2020). Using a multi-user driving simulator system to explore the patterns of vehicle fleet rear-end collisions occurrence under different foggy conditions and speed limits. *Transportation Research Part F*, *74*, 161–172.
Kovakova, J., Bärgman, J., & Dozza, M. (2020). A comparison of computational driver models using naturalistic and test-track data from cyclist-overtaking manoeuvres. *Transportation Research Part F*, *75*, 87–105.
Lakerveld, P. R., Damveld, H. J., Pool, D. M., van der El, K., van Paassen, M. M., & Mulder, M. (2016). The effects of yaw and sway motion cues in curve driving simulation. In *Proceedings of the 13th IFAC/IFIP/IFORS/IEA symposium on analysis, design and evaluation of man-machine systems* (pp. 500–505).
Land, M. F., & Horwood, J. (1995a). Which parts of the road guide steering? *Nature*, *377*, 339–340. https://doi.org/10.1038/377339a0.
Land, M. F., & Horwood, J. (1995b). Which parts of the road guide steering? *Nature*, *377*, 339–340.
Land, M. F., & Horwood, J. (1998). How speed affects the way visual information is used in steering. In A. G. Gale (Ed.), *Vision in vehicles VI* (pp. 43–50). Amsterdam: North Holland.
Land, M. F., & Lee, D. N. (1994). Where we look when we steer. *Nature*, *369*, 742–744.
Levison, W. H., Baron, S., & Kleinman, D. L. (1969). A model for human controller remnant. *IEEE Trans. on Man-Machine Systems*, *10*, 101–108. https://doi.org/10.1109/TMMS.1969.299906.
Li, C., Tang, Y., Zheng, Y., Jayakumar, P., & Ersal, T. (2020). Modeling human steering behavior in teleoperation of unmanned ground vehicles with varying speed. *Human Factors (online)*, *00*, 1–13.
Li, X., Yan, X., & Wong, S. C. (2015). Effects of fog, driver experience and gender on driving behavior on s-curved road segments. *Accident Analysis and Prevention*, *77*, 91–104.
MacAdam, C. C. (2003). Understanding and modeling the human driver. *Vehicle Systems Dynamics*, *40*, 101–134.
Mammer, S., Glaser, S., & Netto, M. (2006). Time to line crossing for lane departure avoidance: A theoretical study and an experimental setting. *IEEE Transactions on Intelligent Transportation Systems*, *7*, 226–241. https://doi.org/10.1109/TITS.2006.874707.
Markkula, G., Boer, E. R., Romano, R., & Merat, N. (2018). Sustained sensorimotor control as intermittent decisions about prediction errors: Computational framework and application to ground vehicle steering. *Biological Cybernetics*, *112*, 181–207. https://doi.org/10.1007/s00422-017-0743-9.
Mars, F. (2008). Driving around bends with manipulated eye-steering coordination. *Journal of Vision*, *8*, 1–11. https://doi.org/10.1167/8.11.10.
McLean, J. R., & Hoffmann, E. R. (1972). The effects of lane width on driver steering control and performance. In *Australian road research board (ARRB) conference* (pp. 418–439).
McLean, J. R., & Hoffmann, E. R. (1973). The effects of restricted preview on driver steering control and performance. *Human Factors*, *15*, 421–430.
McRuer, D. T., Weir, D. H., Jex, H. R., Magdaleno, R. E., & Allen, R. W. (1975). Measurement of driver-vehicle multiloop response properties with a single disturbance input. *IEEE Transactions on Systems, Man and Cybernetics*, *5*, 490–497. https://doi.org/10.1109/TSMC.1975.5408371.
McRuer, D. T., Allen, R. W., Weir, D. H., & Klein, R. H. (1977). New results in driver steering control models. *Human Factors*, *19*, 381–397.
Mole, C. D., Kountouriotis, G., Billington, J., & Wilkie, R. M. (2016). Optic flow speed modulates guidance level control: New insights into two-level steering. *Journal of Experimental Psychology. Human Perception and Performance*, *42*, 1818–1838. https://doi.org/10.1037/xhp0000256.
Mueller, A. S., & Trick, L. M. (2012). Driving in fog: The effects of driving experience and visibility on speed compensation and hazard avoidance. *Accident Analysis and Prevention*, *48*, 472–479.
Mulder, M., & Mulder, J. A. (2005). Cybernetic analysis of perspective flight-path display dimensions. *Journal of Guidance, Control, and Dynamics*, *28*, 398–411.
Mulder, M., Pool, D. M., Abbink, D. A., Boer, E. R., Zaal, P. M. T., Drop, F. M., van der El, K., & van Paassen, M. M. (2018). Manual control cybernetics: State-of-the-art and current trends. *IEEE Transactions on Human-Machine Systems*, *48*, 468–485. https://doi.org/10.1109/THMS.2017.2761342.
Odhams, A. M. C., & Cole, D. J. (2014). Identification of the steering control behaviour of five test subjects following a randomly curving path in a driving simulator. *International Journal of Vehicle Autonomous Systems*, *12*, 44–64.
Padfield, G. D., Lu, L., & Jump, M. (2012). Tau guidance in boundary-avoidance tracking: New perspectives on pilot-induced oscillations. *Journal of Guidance, Control, and Dynamics*, *35*, 80–92.
Rajamani, R. (2011). *Vehicle dynamics and control. Mechanical engineering series*. Springer Science & Business Media.
Reymond, G., Kemeny, A., Droulez, J., & Berthoz, A. (2001). Role of lateral acceleration in curve driving: Driver model and experiments on a real vehicle and a driving simulator. *Human Factors*, *43*, 483–495. https://doi.org/10.1518/001872001775898188.
Rezunenko, E., van der El, K., Pool, D. M., van Paassen, M. M., & Mulder, M. (2018). Relating human gaze and manual control behavior in preview tracking tasks with spatial occlusion. In *Proceedings of the IEEE international conference on systems man, and cybernetics* (pp. 440–3445).
Saleh, L., Chevrel, P., Mars, F., Lafay, J.-F., & Claveau, F. (2011). Human-like cybernetic driver model for lane keeping. In *Proc. of the 18th IFAC world congress* (pp. 4368–4373).
Schnelle, S., Wang, J., Jagacinski, R., & Su, H. (2018). A feedforward and feedback integrated lateral and longitudinal driver model for personalized advanced driver assistance systems. *Mechatronics*, *50*, 177–188.
Siebert, F. W., & Wallis, F. L. (2019). How speed and visibility influence preferred headway distances in highly automated driving. *Transportation Research Part F*, *64*, 485–494.
Ungoren, A. Y., & Peng, H. (2005). An adaptive lateral preview driver model. *Vehicle System Dynamics*, *43*, 245–259.
van der El, K. (2018). *How humans use preview information in manual control* (Ph.D. thesis). Delft University of Technology, Faculty of Aerospace Engineering.
van der El, K., Padmos, S., Pool, D. M., van Paassen, M. M., & Mulder, M. (2018). Effects of preview time in manual control. *IEEE Transactions on Human-Machine Systems*, *48*, 486–495.
van der El, K., Pool, D. M., van Paassen, M. M., & Mulder, M. (2018). Effects of preview on human control behavior in tracking tasks with various controlled elements. *IEEE Transactions on Cybernetics*, *48*, 1242–1252. https://doi.org/10.1109/TCYB.2017.2686335.
van der El, K., Pool, D. M., & Mulder, M. (2019). Measuring and modeling driver steering behavior: From compensatory tracking to curve driving. *Transportation Research. Part F, Traffic Psychology and Behaviour*, *61*, 337–346.

van der El, K., Pool, D. M., van Paassen, M. M., & Mulder, M. (2019). Effects of target trajectory bandwidth on manual control behavior in pursuit and preview tracking. *IEEE Transactions on Human-Machine Systems*, *50*, 68–78.

van der El, K., Pool, D. M., van Paassen, M. M., & Mulder, M. (2020). A unifying theory of driver perception and steering control on straight and winding roads. *IEEE Transactions on Human-Machine Systems*, *50*, 165–175.

van der Hulst, M., Rothengatter, T., & Meijman, T. (1998). Strategic adaptations to lack of preview in driving. *Transportation Research Part F*, *1*, 59–75.

van Paassen, M. M., & Mulder, M. (1998). Identification of human operator control behaviour in multi-loop tracking tasks. In *Proc. of the seventh IFAC/IFIP/IFORS/IEA symposium on analysis, design and evaluation of man-machine systems* (pp. 515–520).

van Winsum, W., & Godthelp, H. (1996). Speed choice and steering behavior in curve driving. *Human Factors*, *38*, 434–441. https://doi.org/10.1518/001872096778701926.

Wang, Z., Zheng, R., Nacpil, E., & Nakano, K. (2022). Modeling and analysis of driver behaviour under shared control through weighted visual and haptic guidance. *IET Intelligent Transport Systems*, *16*, 648–660.

Weir, D. H., & McRuer, D. T. (1970). Dynamics of driver vehicle steering control. *Automatica*, *6*, 87–98. https://doi.org/10.1016/0005-1098(70)90077-4.

Weir, D. H., & McRuer, D. T. (1973). Measurement and interpretation of driver/vehicle system dynamic response. *Human Factors*, *15*, 367–378.

Wolters, J. P. M. A., van der El, K., Damveld, H. J., Pool, D. M., van Paassen, M. M., & Mulder, M. (2018). Effects of simulator motion on driver steering performance with various visual degradations. In *Proc. of the IEEE syst., man and cyb. conf.* (pp. 781–786). IEEE.

Xu, J., Yang, K., Shao, Y., & Lu, G. (2015). An experimental study on lateral acceleration of cars in different environments in Sichuan, southwest China. *Discrete Dynamics in Nature and Society*. https://doi.org/10.1155/2015/494130. Online publication.

Yan, X., Li, X., Liu, Y., & Zhao, J. (2014). Effects of foggy conditions on drivers' speed control behaviors at different risk levels. *Safety Science*, *68*, 275–287.

Zhu, S., & He, Y. (2020). A unified lateral preview driver model for road vehicles. *IEEE Transactions on Intelligent Transportation Systems*, *21*, 4858–4867.

Zolali, M., & Mirbaha, B. (2020). Analysing the effect of foggy weather on drivers' speed choice in two-lane highways. *Proceedings of the Institution of Civil Engineers – Transport*, *173*, 171–183.